Basic Study on Driving Force Control for EVs Using Road Condition Estimation with Machine Learning Image Recognition and Vehicle Dynamics

Tokikazu Mizuguchi, Yuna Morimoto, Binh-Minh Nguyen, Osamu Shimizu, Hiroshi Fujimoto
The University of Tokyo
Kashiwa, Japan
Corresponding author's e-mail: mizuguchi.tokikazu24@ae.k.u-tokyo.ac.jp

***Abstract*—Driving Force Control (DFC) for in-wheel motor electric vehicles has been studied for years. To realize DFC, setting the slip ratio limiter (SRL) through appropriate estimation of the road-tire model is essential on low friction surface. However setting the slip ratio limiter based on vehicle dynamics has faced the issue of tire model estimation delay, a fixed SRL has been commonly used in the traditional DFC. This paper proposes a method to quickly adapt to changes in road conditions by the fusion of vision based SRL estimation with vehicle dynamics based SRL estimation. At the moment of road surface condition transition, the vision-based estimation is referenced to compensate for the delay in the dynamics-based approach using fusion algorithm. Experiments and simulations confirmed an increase in traction force on low friction roads through appropriate setting of slip ratio limiter. Experimental results demonstrated that immediately after a sudden change of road surface condition, the proposed method increased driving force by 15 % compared to conventional DFC systems with a variable SRL based solely on dynamics-based estimation.**

***Index Terms*—Electric vehicles, in-wheel motor, Driving Force Control, Road Friction Estimation, Machine Learning.**

I. Introduction

Due to the growing environmental awareness, electric vehicles (EVs) are becoming increasingly widespread [1], [2]. EVs offer environmental benefits and superior control performance compared to internal combustion engine vehicles, thanks to the merits of electric motors. Such merits include: 1) high torque responsiveness, 2) precise measurement of generated torque through current measurement, and 3) the ability to independently control each wheel enabled by the distributed placement of motors.

Various studies have been conducted worldwide on traction control for EVs [3]–[8]. Driving Force Control (DFC) has been studied for many years as one of the traction control methods, and this study focuses on it. The DFC is designed with a cascade structure, where the outer loop controls the driving force, and the inner loop controls the wheel speed. It is known that the driving force of the wheels can be expressed as a function of the slip ratio λ and the road surface friction coefficient μ. In DFC, it is necessary to estimate the friction coefficient μ between the tire and the road surface and the slip ratio λ when determining the reference wheel speed.

Slip ratio λ and road surface friction μ estimation methods can be broadly categorized into two groups. The former is dynamics-based estimation, which involves using the outputs from motion sensors on the vehicle and estimating with a tire model. This method has the advantage of allowing estimation with high accuracy by using relatively simple algorithms, such as recursive least square (RLS) [5]. Of course, this method can detect the road condition change after it occurs, and it requires precise estimation of the tire model. This field has been extensively researched worldwide over many years [9]–[11]. In some studies, Deep Learning has been used to estimate the tire model [12].

The latter is vision-based estimation. This approach estimates the road condition using image data obtained from sensors such as cameras or Light Detection And Ranging installed on the vehicle [13], [14]. Since this method estimates the road condition directly from image data, it allows detection of road changes before the vehicle encounters them. However, accurately estimating road conditions from image data requires extensive datasets and computational resources, and it is vulnerable to variations in surrounding conditions, such as lighting and weather. This field has seen increasing research interest recently, especially with the rise of autonomous driving studies. Additionally, there has been recent research on the fusion of these two methods [15]–[17].

One advantage of combining these two methods is that when road surface friction changes abruptly, estimation using only Dynamics-Based methods may take time to converge. By incorporating Vision-Based estimation, it is possible to reduce the estimation error between the actual road surface friction and the estimated friction from the Dynamics-Based method until they converge, thus enabling greater driving force.

Although the fusion of dynamics-based and vision-based methods have been recently used for road condition estimation, the estimated value was not utilized for vehicle motion control [15] . Additionally, they either lack detailed descriptions in terms of vehicle motion control [16] or use the simplified road surface condition classifications, which renders them unsuitable for practical applications [17].

In our study, we propose a method that combines predictive vision-based road surface friction estimation using Convo-

lutional Neural Networks (CNN) with precise road surface friction estimation based on vehicle dynamics and apply this approach to actual vehicle motion control. To connect these two estimations, we propose a relationship between driving stiffness and maximum road surface friction based on experimental results. By properly associating the two aforementioned estimation algorithms with low-pass and high-pass filters, a fusion strategy is proposed to update the slip ratio limiter of the driving force control.

The structure of this paper is as follows. The vehicle model is explained in Section II. The setting of the slip ratio limiter based on road surface condition estimation using vehicle dynamics is discussed in Section III, followed by the estimation of the slip ratio limiter based on Vision-based road surface condition estimation in Section IV. Simulations are presented in Section V, with results from real vehicle experiments discussed in Section VI, and conclusions provided in Section VII.

II. Fundamentals of this Study

A. Vehicle Model

As illustrated in Fig.1(a), the equations of rotational motions of wheels and longitudinal motion of vehicles are expressed as follows:

$$J_{\mathrm{ij}}\dot{\omega}_{\mathrm{ij}} = T_i - rF_{d,ij} \tag{1}$$

$$M\dot{V}_{x,\mathrm{i}} = F_{\mathrm{d,fl}} + F_{\mathrm{d,fr}} + F_{\mathrm{d,rf}} + F_{\mathrm{d,rr}} \tag{2}$$

where J denotes the moment of inertia of the wheel, ω is the angular velocity, T is the motor torque, r is the wheel radius, F_d represents the driving force acting on the tire at the contact surface, M is the vehicle mass, and V_{ij} is the vehicle speed. In Fig. 1(a), F_z represents the load on each wheel, which can generally be calculated from the front and rear wheel accelerations a_x and a_y. Here, i indicates the front or rear wheels, and j indicates the left or right wheels. The slip ratio λ is defined by the following equation.

$$\lambda_{\mathrm{ij}} = \frac{V_{\omega,\mathrm{ij}} - V_{x,\mathrm{ij}}}{\max(V_{\omega,\mathrm{ij}}, V_{x,\mathrm{ij}}, \varepsilon)} \tag{3}$$

where $V_\omega = r\omega$, and ε is a small constant to prevent division by zero.

The driving force of the wheels can be expressed as a function of the slip ratio λ and the road surface friction coefficient μ.

$$F_d = \mu(\lambda)F_z \tag{4}$$

The road surface friction coefficient μ and slip ratio λ have a nonlinear relationship which is commonly described by Pacjeka's Magic Formula [18].

$$\mu_i = D\sin\left[C\arctan\left(B\lambda_i - E\left(B\lambda_i - \arctan(B\lambda_i)\right)\right)\right] \tag{5}$$

where B, C, D and E are fitting parameters obtained from experiments [19] and vary depending on the installed tire and road conditions. Generally, the driving stiffness D_s is known to increase in proportion to the maximum road surface friction coefficient μ_{peak}.

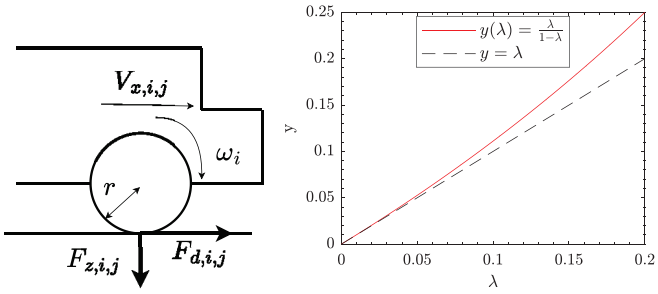

(a) Vehicle model (b) Tire model

Fig. 1. Vehicle model and Tire model

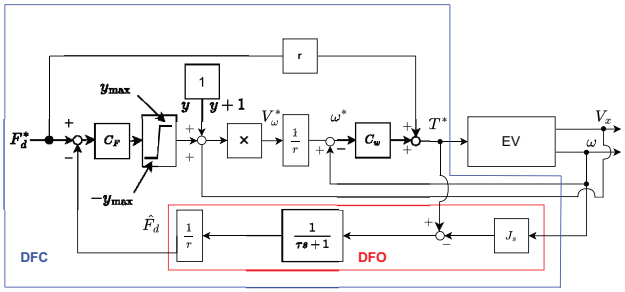

Fig. 2. Block Diagram of Driving Force Controller

Particularly in the region where λ is small, λ and F_d, μ have a linear relationship. Using the slope of this region, known as the driving stiffness D_s, the driving force can be linearized as follows.

$$F_d = D_s\lambda \tag{6}$$

B. Driving Force Controller

This section provides information on the DFC method based on vehicle dynamics [4]–[6]. Fig. 2 shows the block diagram of the driving force control. The outer loop C_f represents the reaction force control, while the inner loop contains the wheel speed control C_ω. F_d^* denotes the target driving force, and $\hat{F}_d$ represents the estimated driving force obtained from Driving Forse Observer (DFO) represented Fig.2.

The slip ratio λ differs in definition between driving ($V_\omega \geq V_x$) and braking ($V_\omega < V_x$), which causes control difficulties. Therefore, instead of the slip ratio, we use the control variable y, defined by the following equation [4]:

$$y = \frac{V_\omega}{V} - 1 \tag{7}$$

This is the same as the definition of the slip ratio λ during braking, and the relationship between y and λ during driving is as follows:

$$y = \frac{\lambda}{1-\lambda} \tag{8}$$

Thus, near $\lambda = 0$, $y \approx \lambda$, and in other regions, there is a one-to-one relationship between the two Fig. 1(b). F_{d} cab be linearized as follows:

$$F_{\mathrm{d}} \simeq D_s\lambda \simeq D_s y \tag{9}$$

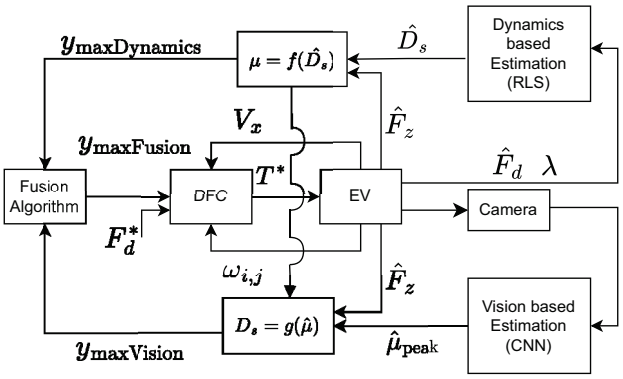

Fig. 3. Proposed DFC System

This demonstrates that y can be utilized as control variable to regulate driving force. Based on (9), y can be utilized as a control variable to control the driving force. C_F can be designed as an integral controller $C_F = K_{fi}/s$ by pole-placement [5].

III. PROPOSAL OF THE CONTROL SYSTEM

A. Overall system

The block diagram of the proposed method in this paper is shown in Fig. 3. This method uses a driving force control method for traction control. The upper-bound $+y_{\max}$ and lower-bound $-y_{\max}$ of the slip ratio limiter is updated by $+y_{\text{maxFusion}}$ and $-y_{\text{maxFusion}}$, respectively, based on vehicle dynamics and image recognition information from machine learning. The goal of this is to maintain maximum driving force on low-friction road surfaces. Estimating the slip ratio limiter based on vehicle dynamics takes approximately $0.5\,\text{s}$ to converge; therefore, by using slip ratio limiter estimation through vision, it is possible to reduce the optimal slip ratio and tracking error to the set slip ratio limiter until the limiter converges.

B. Vehicle Dynamics Based Slip Ratio Limiter

To prevent excessive slip, a limiter is set for y_{max}. This limiter will hereafter be referred to as the slip ratio limiter, defined as follows:

$$y_{\text{maxDynamics}} = \frac{\hat{\mu}_{\text{peak}}\hat{F}_z}{\hat{D}_s} \tag{10}$$

The estimated value of driving stiffness $\hat{D}_s$ is obtained using RLS method [6], [20]. The algorithm for RLS is described as follows. When the output value $y(k)$ is represented as $y(k) = \theta^T \xi(k)$ using an unknown parameter vector $\theta(k)$ and a measurable signal vector $\xi(k)$, the unknown parameter θ can be estimated by Recursive Least Squares as follows:

$$\hat{\theta}(k) = \hat{\theta}(k-1) - \frac{\Gamma(k-1)\xi(k)}{W + \Gamma(k-1)\xi^2(k)} \times \Big(\xi(k)\hat{\theta}(k-1) - y(k)\Big) \tag{11}$$

$$\Gamma(k) = \frac{1}{W}\left(\Gamma(k-1) - \frac{\Gamma^2(k-1)\xi^2(k)}{W + \Gamma(k-1)\xi^2(k)}\right) \tag{12}$$

where, W is the forgetting factor. By associating y, ξ, and θ with F_d, λ, and D_s respectively, the estimated driving stiffness $\hat{D}_s$ can be obtained.

The precision of the estimated value decreases when the signal used in the RLS is small. Consequently, the update of the driving stiffness estimation is halted under these conditions, as expressed in eq.(13). Specifically, when $\xi < \varepsilon_\lambda$, the parameters are maintained as follows:

$$\begin{cases} \theta[k] = \theta[k-1] \\ \Gamma[k] = \Gamma[k-1] \end{cases} \tag{13}$$

here, ε_λ represents a small threshold value.

Using the obtained $\hat{D}_s$, the corresponding value of $\hat{\mu}_{\text{peak}}$ is determined from the pre-acquired $D_s - \mu_{\text{peak}}$ map, and by substituting it into eq. (10), $y_{\text{maxDynamics}}$ can be calculated.

C. Machine Learning Vision Based Slip Ratio Limiter

1) Road Surface Friction Estimation Based On CNN: The slip ratio limiter setting using image recognition based on machine learning is referenced from [13]. This method utilizes CNN and the "Seeing Through Fog Dataset" [21], which contains road friction coefficients and images captured from an onboard camera. The CNN is trained using the Seeing Through Fog Dataset, with images from an onboard camera as input and road friction coefficients as output. The predicted friction coefficient is then converted to the actual tire friction coefficient, $\hat{\mu}_{\text{peak}}$, based on experimental values. In previous studies, the Mean Absolute Error between the estimated maximum road friction coefficient μ_{peak} and the actual maximum road friction coefficient $\hat{\mu}_{\text{peak}}$ was 0.078, and the Root Mean Square Error was 0.132. Similar results were confirmed in the reimplementation [13].

Since the estimated maximum road friction coefficient obtained from camera images represents the estimate in front of the vehicle, the estimated maximum road friction coefficient $\hat{\mu}_{\text{peak}}$ obtained by this method is synchronized with vehicle motion control by considering the following time delay [16].

$$t_{\text{delay}} = \max\left(0, -\Delta t + \int_{P_0}^{P_0+P_1} \frac{1}{V_x}\, dl\right), \tag{14}$$

where, P_1 represents the distance from the center point of the road surface in the image (Preview Position) to the front axle of the vehicle, P_0 is the previous Preview Position represented in Fig.4, and Δt is the time required for image processing.

2) Driving Force Control Based On Image Recognition: Using the maximum road friction coefficient $\hat{\mu}_{\text{peak}}$ obtained by the CNN and the pre-acquired $\mu_{\text{peak}} - D_s$ map, $\hat{D}_s$ is determined, and the slip ratio limiter is defined as follows:

$$y_{\text{maxVision}} = \frac{\hat{\mu}_{\text{peak}}\hat{F}_z}{\hat{D}_s} \tag{15}$$

D. Fusion Algorism Of Slip Ratio Limiters

This section describes the algorithm for integrating the slip ratio limiters $y_{\text{maxDynamics}}$ and $y_{\text{maxVision}}$, which are set based on road condition estimation using vehicle dynamics and image

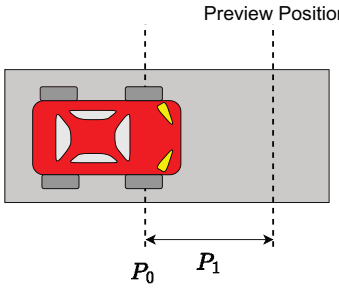

Fig. 4. Preview Position

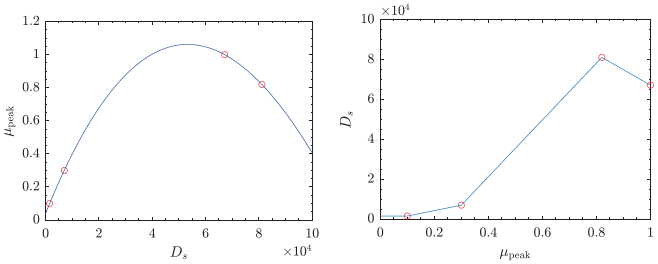

(a) D_s-μ curve (b) μ-D_s curve

Fig. 5. Ds-μ curve and μ-D_s curve

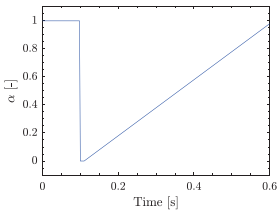

Fig. 6. Variation of α

recognition with machine learning, respectively. The integrated slip ratio limiter is defined as y_{maxALL} and is expressed as follows:

$$y_{\text{maxFusion}} = Q_{\text{LPF}} y_{\text{maxDynamics}} + Q_{\text{HPF}} y_{\text{maxVision}} \tag{16}$$

where, Q_{LPF} and Q_{HPF} are low-pass and high-pass filters, respectively defined as follows:

$$Q_{\text{LPF}} = \frac{\alpha}{1 + \tau_{\text{LPF}} s} \tag{17}$$

$$Q_{\text{HPF}} = 1 - Q_{\text{LPF}} \tag{18}$$

Here, α is a time-varying weight. When the road conditions change, α is set to a small value to prioritize the vision-based slip ratio limiter. After the road conditions have stabilized, α is increased to prioritize the slip ratio limiter based on vehicle dynamics. Furthermore, the time constant τ of the low-pass filter is set to match that of RLS method used for estimating Driving Stiffness D_s.

IV. Simulation Evaluation

A. Simulation Setting

To verify the effectiveness of the proposed method, simulations were conducted. The simulation environment was built using MATLAB/Simulink. In this simulation, the scenario considered a transition in road surface friction coefficient (μ) from 1.0 to 0.3. The estimation of road condition changes using vision is assumed to be 92 % and 108 % accurate following the result of the paper [13]. The μ-D_s curve and D_s-μ curve were provided as shown in Fig. 5 from the experiment [19], and α was varied as shown in Fig. 6. α was varied from 0 to 1 over 0.4 seconds after the road condition change occurred. There are two possible methods for detecting road condition changes: using the time variation of Ds (Case 1) and assuming accurate detection through Vision (Case 2). The commanded value of driving force F_{d} was set to $993\,\text{N}$, and compared with the case where the slip ratio limiter was set based solely on Dynamics estimation. The main parameters are shown in Table I. Communication delays, discretization, and quantization effects were not considered.

B. Simulation Results

Since there was no significant difference in the simulation results between the two cases, only the results for case (2) are presented here to align with the experimental conditions. The simulation results are shown in Figs. 7 and 8. The results indicate that the slip ratio limiter was set appropriately, leading to an increase in both driving force F_d.

V. Experimental Evaluation

Real vehicle experiments were conducted to verify the effectiveness of the proposed method.

A. Experimental Setting

Fig. 9 shows the experimental vehicle, FPEV-2 Kanon. The vehicle is an electric vehicle with four in-wheel motors. The main parameters are shown in Table I.

In this experience, the vehicle was used in a front-wheel-drive system. The experimental setting is shown in Fig. 10, the vehicle first accelerates on a high friction road, and then it enters a low friction road. The commanded value of driving force F_d was set to $400\,\text{N}$. The distance to the road surface change is known, allowing verification that the slip ratio limiter fusion algorithm functions appropriately to maximize driving force. In this experiment, road surface changes are assumed to be known and are not detected by the camera. The results of the proposed method are compared with the case where the slip ratio limiter value is based solely on dynamics-based estimation.

B. Experimental Results

The experimental results are shown in Fig. 11 and 12. In Fig. 12(d) The blue line represents the slip ratio limiter integrated from both Vision and Dynamics, while the red line represents the slip ratio limiter based only on Dynamics. The red vertical line indicates the boundary between high friction and low friction surfaces. The results indicate that SRL was set appropriately, leading to an increase driving force F_d. Compared to the case where conventional DFC system with a

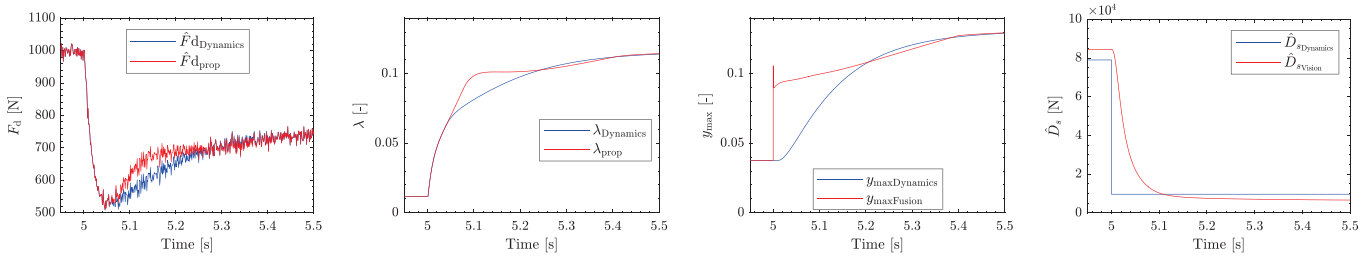

(a) Driving force (b) Slip ratio (c) Slip ratio limiter (d) Estimated Driving Stiffness

Fig. 7. Simulation results of case(2) when the estimation accuracy of Vision was 108 %

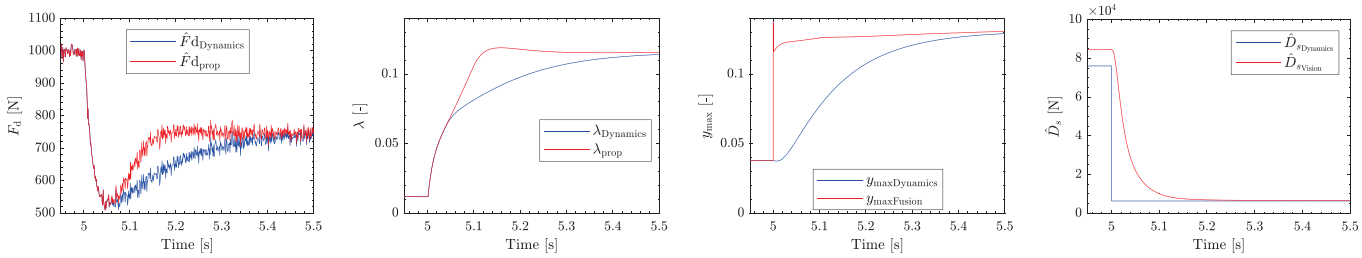

(a) Driving force (b) Slip ratio (c) Slip ratio limiter (d) Estimated Driving Stiffness

Fig. 8. Simulation results of case(2) when the estimation accuracy of Vision was 92 %

TABLE I
MAIN PARAMETERS

Symbol	Description	Value
M	Vehicle mass	925 kg
r	Wheel Radius	0.302 m
J	Wheel Inertia	1.24 kg m^2

Fig. 9. FPEV-2 Kanon

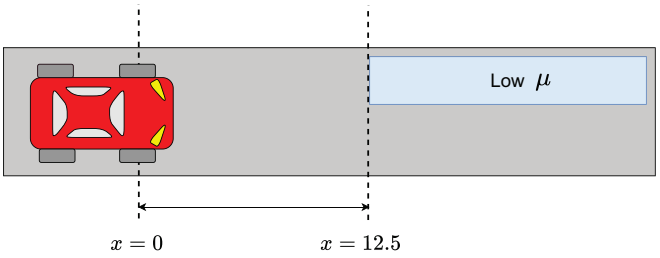

Fig. 10. Experimental Setting

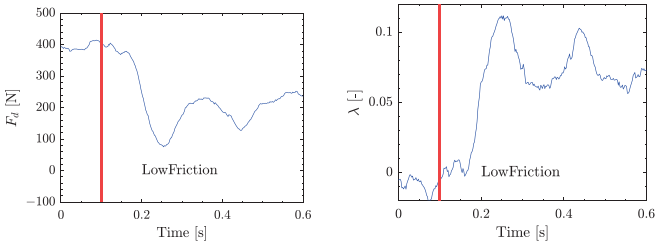

(a) Driving force (b) Slip ratio

Fig. 11. Experimental results of conventional method with variable SRL solely based on Dynamics estimation

variable SRL based solely on dynamics-based estimation, the average driving force over the 0.5 s following the road condition change increased from 223 N to 241 N. In particular, the average driving force at 0.4 s seconds after 0.2 seconds, when $y_{maxFusion}$ is larger than $y_{maxDynamics}$, increased from 187 N to 216 N (Fig.13). Here, the reason why the experimental results did not show a large increase in driving force compared to the simulation is due to the delay in responsiveness of the DFC itself caused by the delay of the sensors mounted on the actual vehicle. If a driving force control method with even faster response is proposed in the future, the effectiveness of the proposed method will be further enhanced.

VI. CONCLUSION

In this paper, we propose a method to enhance driving force on low friction road surfaces by optimally setting the slip ratio limiter in conventional Driving Force Controllers. This method can combine predictive, vision-based road surface friction estimation using CNN with precise road surface friction estimation based on vehicle dynamics. Experimental results

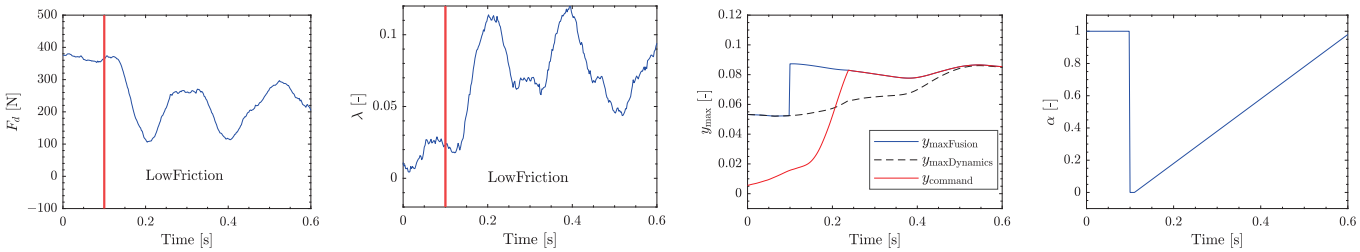

(a) Driving force (b) Slip ratio (c) Slip ratio limiter (d) Variation of α

Fig. 12. Experimental results of proposed method with variable SRL based on Vision and Dynamics estimation

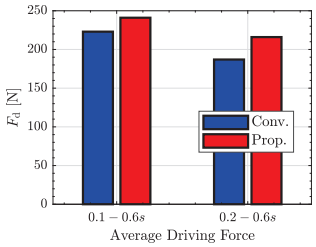

Fig. 13. Driving force comparison

showed that the proposed method increased driving force by 15 % compared to conventional DFC systems with a variable SRL based solely on dynamics based estimation. In the future, we plan to implement a comprehensive system that consistently detects road surface condition changes, estimates road surface friction coefficients, and controls driving force accordingly.

ACKNOWLEDGMENT

This research was partly supported by Industrial Technology Research Grant Program from New Energy and Industrial Technology Development Organization (NEDO) of Japan (number 05A48701d), the Ministry of Education, Culture, Sports, Science and Technology grant (number 22246057 and 26249061)

REFERENCES

[1] R. Irle, "Global EV sales for 2022," 2023.

[2] S. Oki and Y. Sato, "Nissan LEAF and e-POWER: Evolution of motors and inverters," *IEEJ J. Ind. Appl.*, vol. 13, no. 23006552, pp. 8–16, 2023.

[3] V. Ivanov, D. Savitski, and B. Shyrokau, "A survey of traction control and antilock braking systems of full electric vehicles with individually controlled electric motors," *IEEE Trans. Veh. Technol.*, vol. 64, no. 9, pp. 3878–3896, Sep. 2015.

[4] M. Yoshimura and H. Fujimoto, "Driving torque control method for electric vehicle with in-wheel motors," *Electr. Eng. Japan*, vol. 181, no. 3, pp. 49–58, Nov. 2012.

[5] K. Maeda, H. Fujimoto, and Y. Hori, "Four-wheel driving-force distribution method based on driving stiffness and slip ratio estimation for electric vehicle with in-wheel motors," in *2012 IEEE Vehicle Power and Propulsion Conference*. IEEE, Oct. 2012, pp. 1286–1291.

[6] J. Amada and H. Fujimoto, "Torque based direct driving force control method with driving stiffness estimation for electric vehicle with in-wheel motor," in *IECON 2012 - 38th Annual Conference on IEEE Industrial Electronics Society*. IEEE, Oct. 2012.

[7] B.-M. Nguyen, T. Kobayashi, K. Sekitani, M. Kawanishi, and T. Narikiyo, "Altitude control of quadcopters with absolute stability analysis," *IEEJ J. Ind. Appl.*, vol. 11, no. 4, pp. 562–572, Jul. 2022.

[8] N. Wada and Y. Matsui, "Driving force control for a vehicle considering slip ratio limitation: DRIVING FORCE CONTROL FOR a VEHICLE," *IEEJ Trans. Electr. Electron. Eng.*, vol. 14, no. 2, pp. 297–302, Feb. 2019.

[9] R. Hoseinnezhad and A. Bab-Hadiashar, "Efficient antilock braking by direct maximization of Tire–Road frictions," *IEEE Trans. Ind. Electron.*, vol. 58, no. 8, pp. 3593–3600, Aug. 2011.

[10] B.-M. Nguyen, S. Hara, H. Fujimoto, and Y. Hori, "Slip control for IWM vehicles based on hierarchical LQR," *Control Eng. Pract.*, vol. 93, p. 104179, Dec. 2019.

[11] H. Fujimoto, T. Saito, A. Tsumasaka, and T. Noguchi, "Motion control and road condition estimation of electric vehicles with two in-wheel motors," in *Proceedings of the 2004 IEEE International Conference on Control Applications, 2004.*, vol. 2. IEEE, 2004, pp. 1266–1271 Vol.2.

[12] R. Marotta, V. Ivanov, S. Strano, M. Terzo, and C. Tordela, "Deep learning for the estimation of the longitudinal slip ratio," in *2023 IEEE International Workshop on Metrology for Automotive (MetroAutomotive)*. IEEE, Jun. 2023, pp. 193–198.

[13] R. Ojala and A. Seppänen, "Lightweight regression model with prediction interval estimation for computer vision-based winter road surface condition monitoring," *IEEE Transactions on Intelligent Vehicles*, vol. PP, no. 99, pp. 1–13.

[14] S. Roychowdhury, M. Zhao, A. Wallin, N. Ohlsson, and M. Jonasson, "Machine learning models for road surface and friction estimation using Front-Camera images," in *2018 International Joint Conference on Neural Networks (IJCNN)*. IEEE, Jul. 2018, pp. 1–8.

[15] Z. Du, A. Skar, M. Pettinari, and X. Zhu, "Pavement friction evaluation based on vehicle dynamics and vision data using a multi-feature fusion network," *Transp. Res. Rec.*, vol. 2677, no. 11, pp. 219–236, Nov. 2023.

[16] B. Leng, D. Jin, X. Hou, C. Tian, L. Xiong, and Z. Yu, "Tire-Road peak adhesion coefficient estimation method based on fusion of vehicle dynamics and machine vision," *IEEE Trans. Intell. Transp. Syst.*, vol. 23, no. 11, pp. 21 740–21 752, Nov. 2022.

[17] T. Ueno, H. Pousseur, B. M. Nguyen, A. C. Victorino, and H. Fujimoto, "Proposal of on-board Camera-Based driving force control method for autonomous electric vehicles," in *2023 IEEE/ASME International Conference on Advanced Intelligent Mechatronics (AIM)*. IEEE, Jun. 2023, pp. 424–429.

[18] H. B. Pacejka and E. Bakker, "The magic formula tyre model," *Veh. Syst. Dyn.*, vol. 21, no. sup001, pp. 1–18, Jan. 1992.

[19] MathWorks, "Tire-road interaction (magic formula)," 2023, accessed: 2024-11-03. [Online]. Available: https://jp.mathworks.com/help/sdl/ref/tireroadinteractionmagicformula.html

[20] C. Ge, B.-M. Nguyen, H. Fujimoto, Y. Terada, and M. Sakamoto, "Multirate adaptive robust control with friction estimation and compensation for tilting table machine tools," in *2024 IEEE 18th International Conference on Advanced Motion Control (AMC)*. IEEE, Feb. 2024, pp. 1–6.

[21] M. Bijelic, T. Gruber, F. Mannan, F. Kraus, W. Ritter, K. Dietmayer, and F. Heide, "Seeing through fog without seeing fog: Deep multimodal sensor fusion in unseen adverse weather," in *2020 IEEE/CVF Conference on Computer Vision and Pattern Recognition (CVPR)*. IEEE, Jun. 2020.